Dynamic polarizabilities and hyperfine-structure constants for Sc^{2+}

Narendra Nath Dutta,[1] Sourav Roy,[2] and P. C. Deshmukh[1]
[1]*Department of Physics, Indian Institute of Technology Madras, Chennai-600036, India*
[2]*Department of Physics, Indian Institute of Technology Kharagpur, Kharagpur-721302, India*
(Received 30 July 2015; published 6 November 2015)

In this work, we calculate dynamic polarizabilities and hyperfine-structure A and B constants of a few low-lying states for Sc^{2+}. The sum-over-states technique is applied to calculate the polarizabilities of the $3d\ ^2D_{3/2}$, $3d\ ^2D_{5/2}$, and $4s\ ^2S_{1/2}$ states. The most important and correlation sensitive part of the sum is calculated using a highly correlated relativistic coupled-cluster theory. The remaining part of the sum is calculated using a lower-order many-body perturbation theory and the Dirac-Fock theory. Present dynamic polarizabilities are important to investigate the Stark shifts in the $4s\ ^2S_{1/2}$–$3d\ ^2D_{5/2}$ and $4s\ ^2S_{1/2}$–$3d\ ^2D_{3/2}$ clock transitions of Sc^{2+}. Magic wavelengths for zero Stark shifts corresponding to these transitions are found in the vacuum-ultraviolet region. The coupled-cluster theory is used to estimate the hyperfine A and B constants with a very high accuracy.

DOI: 10.1103/PhysRevA.92.052510 PACS number(s): 31.15.ap, 33.15.Pw, 31.15.xp, 31.15.bw

I. INTRODUCTION

Proposals of using atomic clocks in the optical region of the electromagnetic spectrum open up the curiosity to investigate the transitions between the electronic energy levels of several atoms and ions [1–3]. It has been proposed and observed that with respect to the neutral atomic species, ions can provide more accurate clock transition frequencies [2–8]. Some optical transitions of several ions, starting from singly charged to multiply charged, have made them excellent candidates of atomic clocks in the past two decades [2–6]. In the literature, there are a number of indications of using the forbidden transition between a ground state or a very long-lived metastable state and a higher excited state of an ion as clock transition [2,3,8–13]. Along this direction, we find that the optical transitions between the second excited state $4s\ ^2S_{1/2}$ and the first excited state $3d\ ^2D_{5/2}$, the ground state $3d\ ^2D_{3/2}$ of Sc^{2+} can be used as clock transitions. The wavelengths for $4s\ ^2S_{1/2}$–$3d\ ^2D_{5/2}$ and $4s\ ^2S_{1/2}$–$3d\ ^2D_{3/2}$ transitions of this ion are 3946.07 Å and 3915.53 Å, respectively [14]. The lifetime of the metastable state $4s\ ^2S_{1/2}$ is around 0.05 s [15]. The lifetime of the first excited state $3d\ ^2D_{5/2}$ is very large, about 1.2×10^4 s [15], and hence it can be treated as a very long-lived metastable state. The cooling transitions $3d\ ^2D_{3/2,5/2} \rightarrow 4p\ ^2P_{1/2,3/2}$ of this ion can be operable by a tunable coherent source in the VUV region [16–21]. Therefore, this ion has the necessary features to be applicable as a possible candidate of an optical atomic clock.

However, any transition suffers shifts due to the presence of external perturbations [22]. Such perturbations arise mainly from the blackbody radiation due to nonzero room temperature [22–25] and from external electric field used to trap the ion [22,26]. Such trapping field can cause Stark shifts in the energy levels and hence in the clock transition frequencies associated with these levels [22,26]. As a result, the accuracy of a clock frequency is reduced. Therefore, corrections should be made to account for this type of electric-field-induced shifts. This requires estimations of the electric dipole polarizabilities of the clock transition states, as the Stark shifts are proportional to these polarizabilities and intensity of the applied electric field [22]. Laser cooling and trapping of ions were proposed, studied, and have been demonstrated [27–29] already. Ions having a single valence electron were studied for laser trapping recently [27].

The electric dipole polarizability of an atom or ion depends on the frequency of an applied electric field [22,26]. As a consequence, the Stark shift is also frequency dependent or dynamic in nature. It is usual that with changing frequency of a tunable laser, one can see changes in the Stark shifts of different energy levels and hence in the transition energies among them. Therefore, the clock frequency shift due to such dynamic effect should be considered. Nevertheless, such study can also select some frequencies of a tunable radiation source where the polarizabilities and consequently the Stark shifts corresponding to transition states become equal [26]. As a result, the transition energy between two such states remains unaffected by the electric field due to such choices of the source frequencies. The wavelengths corresponding to these frequencies are called magic wavelengths [22,26]. For an atom or ion, sometimes these wavelengths are useful to determine transition strengths of a few specific transitions or ratios between them [22,26]. The blackbody radiation shift of a clock frequency is proportional to the difference of the zero-frequency scalar polarizabilities of the clock transition states [22,23].

Scandium in its neutral and different ionized states is abundant in various stellar media [30–36]. There are evidences of the presence of Sc in various astrophysical systems, such as solar atmosphere [30], ζ Oph cloud [30], disk and metal-rich halo stars [32], planet-host stars [36], Am stars [34], etc. As a consequence, the transition parameters of Sc and its different ions have been a matter of considerable research interest in the past four decades [31,37–44]. Especially, a few reports are available in the literature on the issues of abundance anomalies of Sc, which demand careful line-profile analysis using accurate hyperfine data [32,39,40,45]. In this regard, results on hypefine parameters are available for neutral Sc [40] and singly ionized Sc [39,46]. The present work on the hyperfine values for the Sc^{2+} ion is a supply to these parameters in the literature.

In the present work, we perform calculations on the dynamic electric dipole polarizabilities and hyperfine structure A and B constants for Sc^{2+}. Here the total polarizabilities are divided in two parts: core and valence parts. Each of these

two parts is calculated using the sum-over-states approach as described in Ref. [22]. In the valence part of a polarizability, the most dominant contribution to the sum is calculated using the relativistic coupled-cluster theory with single, double, and partial valence triple excitations [RCCSD(T)] in linear and nonlinear forms [47]. In this part, the remaining contribution to the sum is evaluated using the second-order relativistic many-body perturbation theory [RMBPT(2)] [48] and the Dirac-Fock (DF) theory. RMBPT(2) is also used to estimate the core polarizability of the Sc^{3+} ionic core. Additionally, we calculate the total polarizabilities (valence + core) using only the Dirac-Fock wave functions to see the changes in these values with the correlation corrections to the wave functions. The *ab initio* correlation corrected results are improved further by the inclusion of the experimental transition energies in the valence part. We consider the frequency dependence not only in the valence part but also in the core part of a polarizability. The present RCCSD(T) theory, as mentioned above, is employed also to estimate the hyperfine structure A and B constants to a very high accuracy.

II. THEORY

The coupled-cluster theory for a single-valence system is explained in detail in Refs. [48–51]. Briefly, this theory relates a single-valence correlated atomic state $|\Psi_v\rangle$ with its corresponding DF reference state $|\Phi_v\rangle$ using the relation

$$|\Psi_v\rangle = e^T\{1 + S_v\}|\Phi_v\rangle, \tag{2.1}$$

where "v" denotes the orbital in which the valence electron is considered. Here T and S_v are the cluster operators that produce excitations with respect to the closed-shell core and the single-valence open shell, respectively.

The dynamic or frequency-dependent Stark shift of an atomic energy level that depends quadratically on the electric field can be written as [22]

$$F(\omega) = -\tfrac{1}{2}\alpha(\omega)E^2, \tag{2.2}$$

where $\alpha(\omega)$ is the polarizability of the system at frequency ω and E is the magnitude of the applied electric field.

The present method for calculation of the total dynamic polarizability of a system is described well in Ref. [22]. For a single-valence atomic system having a valence electron in the vth orbital, this polarizability can be represented as

$$\alpha(\omega) = \alpha(\omega)_c + \alpha(\omega)_v + \alpha(\omega)_{vc}. \tag{2.3}$$

This polarizability reduces to the static form for $\omega \to 0$. Here, $\alpha(\omega)_c$ is the core polarizability of the ionic core. This ionic core is obtained by removing the valence electron from the system. With such a consideration, α_{vc} provides the correction term to the core polarizability due to the presence of the valence electron. As the core electrons are tightly bound to the nucleus, the presence of a valence electron is expected to change the core polarizability by little amount [24]. Thus we consider $\alpha(\omega)_{vc}$ in the present method of calculations, but its ω dependency is neglected. $\alpha(\omega)_v$ is the valence polarizability of the single-valence system. It is very much sensitive to correlation correction due to reduced binding of the valence electron to the nucleus.

In order to estimate the core polarizability, we use the following expression [22,52,53]:

$$\alpha(\omega)_c = \frac{2}{3}\sum_{ap}\frac{|\langle\Phi_a||d_{\rm DF}||\Phi_p\rangle\langle\Phi_a||d_{\rm RMBPT(2)}||\Phi_p\rangle|(\varepsilon_p - \varepsilon_a)}{(\varepsilon_p - \varepsilon_a)^2 - \omega^2}. \tag{2.4}$$

Here a represents all the core orbitals. p represents all virtual orbitals of appropriate symmetries with respect to these core orbitals. We calculate the core polarizability at the DF level replacing $\langle\Phi_a||d_{\rm RMBPT(2)}||\Phi_p\rangle$ in the numerator of Eq. (2.4) by $\langle\Phi_a||d_{\rm DF}||\Phi_p\rangle$.

The valence part of the polarizability is contributed by a scalar part and a tensor part following the relation [22]

$$\alpha(\omega)_v = \alpha(\omega)_v^{(0)} + \frac{3M_v^2 - J_v(J_v+1)}{J_v(2J_v-1)}\alpha(\omega)_v^{(2)}, \tag{2.5}$$

where $\alpha(\omega)_v^{(0)}$ and $\alpha(\omega)_v^{(2)}$ determine the scalar and tensor parts, respectively. Here J_v is the total angular momentum of the state $|\Psi_v\rangle$, while M_v is its magnetic component. Using the sum-over-states form, the mathematical expressions for $\alpha(\omega)_v^{(0)}$ and $\alpha(\omega)_v^{(2)}$ can be written as [22]

$$\alpha(\omega)_v^{(0)} = \frac{2}{3(2J_v+1)}\sum_n \frac{|\langle\Psi_v||d||\Psi_n\rangle|^2 \times (E_n - E_v)}{(E_n - E_v)^2 - \omega^2} \tag{2.6}$$

and

$$\alpha(\omega)_v^{(2)} = 4\left(\frac{5J_v(2J_v-1)}{6(J_v+1)(2J_v+1)(2J_v+3)}\right)^{1/2} \times \sum_n\left[(-1)^{J_v+J_n}\begin{Bmatrix} J_v & 1 & J_n \\ 1 & J_v & 2\end{Bmatrix} \times \frac{|\langle\Psi_v||d||\Psi_n\rangle|^2(E_n - E_v)}{(E_n - E_v)^2 - \omega^2}\right]. \tag{2.7}$$

The hyperfine shift of an atomic energy level associated with the hyperfine quantum number F can be approximated by the following expression [54]:

$$H_{\rm hfs} = \frac{AK}{2} + \frac{1}{2}\frac{3K(K+1) - 4J_v(J_v+1)I(I+1)}{2I(2I-1)2J_v(2J_v-1)}B. \tag{2.8}$$

$K = F(F+1) - I(I+1) - J_v(J_v+1)$, and A and B are magnetic dipole and electric quadrupole hyperfine constants, respectively. The justification for the approximation comes from the fact that, in general, there are very few contributions from the higher-order moments beyond the magnetic dipole and the electric quadrupole moments, such as the magnetic octupole moment of the nucleus, that can occur in $H_{\rm hfs}$. The mathematical forms to represent the A and B constants are given as [54]

$$A = \mu_N g_I \frac{\langle J_v||\mathbf{T}^{(1)}||J_v\rangle}{\sqrt{J_v(J_v+1)(2J_v+1)}} \tag{2.9}$$

and

$$B = 2eQ\sqrt{\frac{2J_v(2J_v-1)}{(2J_v+1)(2J_v+2)(2J_v+3)}}\langle J_v||\mathbf{T}^{(2)}||J_v\rangle, \tag{2.10}$$

where μ_N is the nuclear magneton and Q is the electric quadrupole moment of the nucleus; g_I is the g factor of

TABLE I. Comparison of the dipole matrix elements (reduced form) in a.u. with the present and other calculations (Other). The values in parentheses indicate the uncertainties in the present calculations.

Transitions	DF	Present	Other[a]	Other[b]
$4s\ ^2S_{1/2}$–$4p\ ^2P_{1/2}$	2.582	2.344 (±0.2%)	2.345	2.331
$4s\ ^2S_{1/2}$–$4p\ ^2P_{3/2}$	3.652	3.316 (±0.2%)	3.318	3.298
$3d\ ^2D_{3/2}$–$4p\ ^2P_{1/2}$	1.536	1.321 (±1.1%)	1.325	1.320
$3d\ ^2D_{3/2}$–$4p\ ^2P_{3/2}$	0.683	0.588 (±1.1%)	0.589	0.588
$3d\ ^2D_{3/2}$–$4f\ ^2F_{5/2}$	1.401	1.165 (±0.4%)	1.173	1.157
$3d\ ^2D_{5/2}$–$4p\ ^2P_{3/2}$	2.056	1.771 (±1.1%)	1.780	1.770
$3d\ ^2D_{5/2}$–$4f\ ^2F_{5/2}$	0.376	0.313 (±0.4%)	0.315	0.311
$3d\ ^2D_{5/2}$–$4f\ ^2F_{7/2}$	1.679	1.399 (±0.4%)	1.411	1.390

[a]Reference [44].
[b]Reference [15].

the nucleus and is represented by $g_I = \frac{\mu_I}{I}$, where μ_I is the magnetic moment of the nucleus in the unit of nuclear magnetons. The reader is referred to Ref. [54] for detailed explanations of the above two mathematical expressions.

III. RESULTS AND DISCUSSIONS

We start our calculations with generating the DF orbital basis functions having two-parameters Gaussian type form [55]. These parameters are optimized with respect to the energies and radial wave functions of the DF orbitals obtained using the GRASP92 code of Parpia *et al.* [56]. We use 35, 32, 25, 22, and 20 basis functions for the s, p, d, f, and g symmetries, respectively, at the DF level of calculations. The number of active orbitals (including all the core orbitals) considered for these symmetries during the RCCSD(T) and RMBPT(2) calculations is 12, 11, 10, 9, and 8, respectively. We have tested that these large numbers of symmetries and active orbitals are sufficient to include the correlation corrections in the energies, dipole matrix elements, and hyperfine constants without too much computational complexity [55]. We compare the most important dipole matrix elements in reduced forms as calculated by the present RCCSD(T) method with the corresponding CCSDpT results of Nandy *et al.* [44] and SDpT results of Safronova *et al.* [15] in Table I. The CCSDpT results were calculated in a similar way as the RCCSD(T) results are calculated by us. The small differences between these two sets of results may be the consequence of different choices of optimized parameters for the basis functions, and the consideration of different numbers of active orbitals used in the coupled-cluster calculations. The SDpT values are calculated using the single, double, and partial triple excitations, but in a linearized form. In this form, they used a linear approximation: $|\Psi_v\rangle \approx \{1 + T + S_v\}|\Phi_v\rangle$ in Eq. (2.1). However, inclusion of nonlinear terms, such as $\frac{T^2}{2!}$, is more appropriate theoretically [47,57], and is considered in the present work. We have estimated the uncertainties in our results which arise from the neglect of Breit interaction and some of the quantum electrodynamics (QED) effects, as well as the limited number of active orbitals and symmetries.

In Eq. (2.6) and Eq. (2.7), the set of intermediate states (the running label "n" in the summation) which can provide nonzero dipole matrix elements in the calculations of the valence polarizabilities of $4s\ ^2S_{1/2}$, $3d\ ^2D_{3/2}$, and $3d\ ^2D_{5/2}$ states are $\{np\ ^2P_{1/2},\ np\ ^2P_{3/2}\}$, $\{np\ ^2P_{1/2},\ np\ ^2P_{3/2},\ nf\ ^2F_{5/2}\}$, and $\{np\ ^2P_{3/2},\ nf\ ^2F_{5/2},\ nf\ ^2F_{7/2}\}$, respectively. For both the equations, we consider the sums up to $n = 25$. The terms with $n > 25$ were found to contribute very little. The sum of the terms having $n = 4$, 5, and 6 for $np\ ^2P_{1/2,3/2}$ states and $n = 4$, 5 for $nf\ ^2F_{5/2,7/2}$ states contribute dominantly and are sensitive to correlation correction. Therefore, calculations of these parts of the sums need exhaustive treatment of the correlation correction which is performed here using the RCCSD(T) [49] wave functions. We define these parts as Part I. We consider the next significant contributions in the sums up to $n = 12$ for the $np\ ^2P_{1/2,3/2}$ and $nf\ ^2F_{5/2,7/2}$ states. In these parts, the dipole matrix elements are calculated by including core polarization correction on top of the DF approximation using the RMBPT(2) [53]. We define these parts as Part II. The remaining parts of the sums with $n = 13$ to $n = 25$ contribute marginally, and are thus determined using the DF wave functions. We label these parts as Part III.

TABLE II. Values of static dipole polarizabilities in a.u. at the various levels of calculations. The values in parentheses indicate the uncertainties in the present calculations.

State		DF	CC	CC (Expt.)
$4s\ ^2S_{1/2}$	Scalar	43.73	35.07	35.23 (±1%)
$3d\ ^2D_{3/2}$	Scalar	5.10	4.02	4.00 (±5%)
	Tensor	−1.63	−1.03	−1.02 (±3%)
$3d\ ^2D_{5/2}$	Scalar	5.08	4.03	4.01 (±5%)
	Tensor	−2.30	−1.47	−1.45 (±3%)

In Table II, we present static values of scalar $[\alpha(\omega)_v^{(0)} + \alpha(\omega)_c + \alpha(\omega)_{vc}]$ and tensor $[\alpha(\omega)_v^{(2)}]$ polarizabilities calculated using different approaches. Here the column labeled by DF shows the results when all the Part I, Part II, and Part III of $\alpha(\omega)_v$ along with $\alpha(\omega)_c$ and $\alpha(\omega)_{vc}$ are calculated using the DF wave functions only. The CC represents the results where $\alpha(\omega)_c$ and $\alpha(\omega)_{vc}$ are treated with RMBPT(2), and the correlation corrections in Part I and Part II of $\alpha(\omega)_v$ are included as described in the previous paragraph but Part III of $\alpha(\omega)_v$ is calculated at the DF level. Based on the CC results, the CC(Expt.) results are obtained by replacing the RCCSD(T) energies in the denominators of Eq. (2.6) and Eq. (2.7) by the experimental transition energies from the National Institute of Standards and Technology (NIST) [14]. Such replacements are seen to change the CC polarizabilities by a small amount. However, the CC(Expt.) polarizabilities are recommended and their uncertainties are discussed in the later part of this section. Nevertheless, the correlation corrections to the wave functions are crucial in calculating the polarizabilities at a desired level of accuracy. These corrections reduce the magnitudes of the scalar polarizabilities by about 20% to 21% and tensor polarizabilities by about 36% to 37%.

The frequency dependencies of the total polarizabilities $[\alpha(\omega)]$ for the $4s\ ^2S_{1/2}$, $3d\ ^2D_{3/2}$, and $3d\ ^2D_{5/2}$ states are plotted in Fig. 1, Fig. 2, Fig. 3, Fig. 4, Fig. 5, and Fig. 6 for the different magnetic sublevels as indicated therein. The plots are made using the polarizability values for frequencies

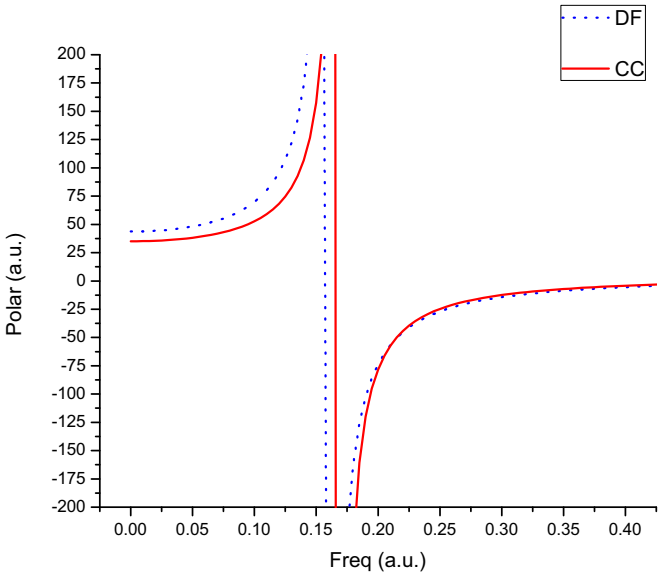

FIG. 1. (Color online) Frequency (Freq) dependence of polarizability (Polar) for the $4s\ ^2S_{1/2}$ state.

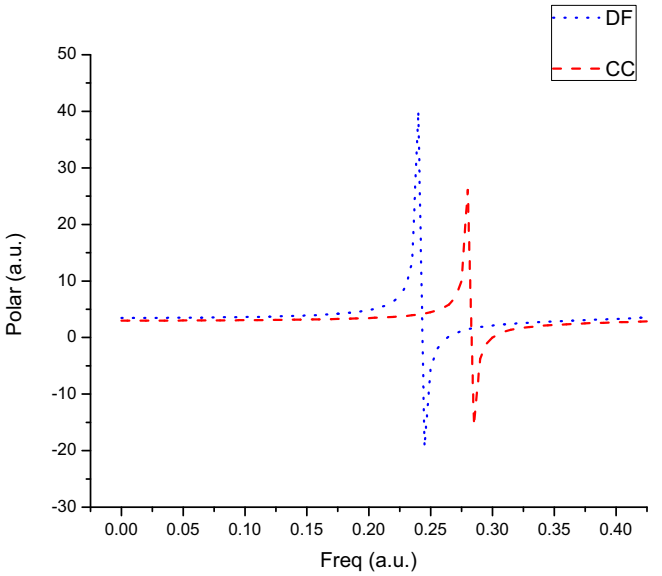

FIG. 3. (Color online) Frequency (Freq) dependence of polarizability (Polar) for the $3d\ ^2D_{3/2}$ state with $M = \pm 3/2$.

from $\omega = 0$ a.u. to $\omega = 0.425$ a.u. with a frequency interval of $\Delta\omega = 0.005$ a.u. In each of these plots, the polarizability values at both the DF and CC levels, as described in the previous paragraph, are shown. The resonances in these plots correspond to the first excitation energies. Their appearances can be understood from the energy denominators in Eq. (2.6) and Eq. (2.7). For the $4s\ ^2S_{1/2}$, $3d\ ^2D_{3/2}$, and $3d\ ^2D_{5/2}$ states, the resonances happen due to the $4s\ ^2S_{1/2} - 4p\ ^2P_{1/2,3/2}$, $3d\ ^2D_{3/2} - 4p\ ^2P_{1/2,3/2}$, and $3d\ ^2D_{5/2} - 4p\ ^2P_{3/2}$ transitions, respectively. The energies corresponding to these transitions are represented in Table III. With increasing ω, the resonances appear at the positive side of the polarizabilities. At the left side of the resonances, the polarizabilities remain positive and increase with increasing frequency. At higher ω value of this side, a higher value of a polarizability and hence an induced dipole moment indicates a valence electron is more loosely bound to the nucleus. The impacts of the correlation corrections to the wave functions make the ω sensitive regions for the $3d\ ^2D_{3/2}$ and $3d\ ^2D_{5/2}$ states with $M = \pm 1/2, \pm 3/2$ blueshifted. These shifts appear to be nearly equal to the differences of the first excitation energies calculated using the DF and the RCCSD(T) theories. The ω sensitive region for the $4s\ ^2S_{1/2}$ state also gets blueshifted by the correlation. But this shift is comparatively small with respect to the shifts in the case of the $3d\ ^2D_{3/2}$ and $3d\ ^2D_{5/2}$ states as mentioned before. It can be understood as a consequence of the larger amount

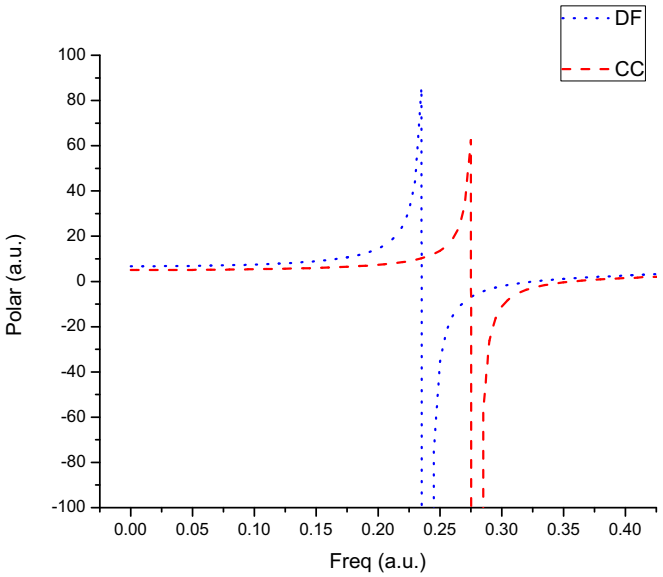

FIG. 2. (Color online) Frequency (Freq) dependence of polarizability (Polar) for the $3d\ ^2D_{3/2}$ state with $M = \pm 1/2$.

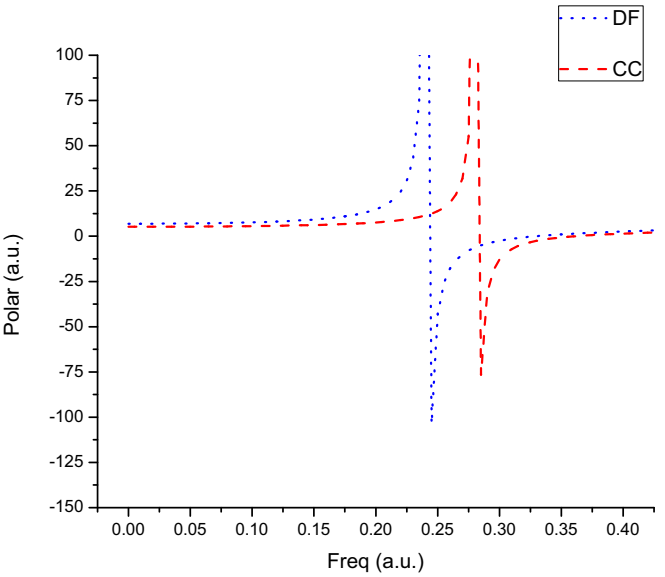

FIG. 4. (Color online) Frequency (Freq) dependence of polarizability (Polar) for the $3d\ ^2D_{5/2}$ state with $M = \pm 1/2$.

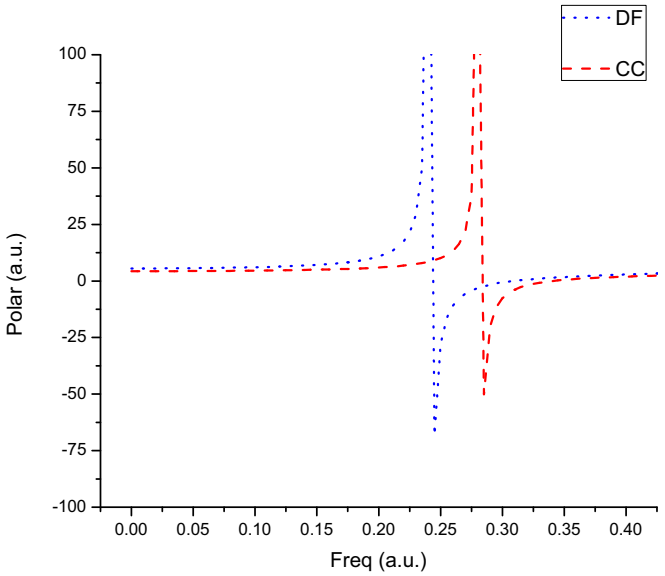

FIG. 5. (Color online) Frequency (Freq) dependence of polarizability (Polar) for the $3d\ ^2D_{5/2}$ state with $M = \pm 3/2$.

of correlation corrections to the $3d\ ^2D_{3/2,5/2} \rightarrow 4p\ ^2P_{1/2,3/2}$ transitions compared to those to the $4s\ ^2S_{1/2} \rightarrow 4p\ ^2P_{1/2,3/2}$ transitions. The $M = \pm 5/2$ component of the $3d\ ^2D_{5/2}$ state shows no resonance at both levels of calculations. For this component, we have found a strong cancellation between the scalar and tensor parts of the polarizability at every value of ω.

We compare the frequency versus total polarizability plots at the CC level for the $4s\ ^2S_{1/2}$ and $3d\ ^2D_{3/2}$ states in Fig. 7, and for the $4s\ ^2S_{1/2}$ and $3d\ ^2D_{5/2}$ states in Fig. 8. From these plots, one can observe that the differences between the polarizabilities of the $4s\ ^2S_{1/2}$ and $3d\ ^2D_{3/2,5/2}$ states in the region $\omega = 0$ a.u. to $\omega = 0.125$ a.u. can cause noticeable Stark shifts in the optical transitions $4s\ ^2S_{1/2} \rightarrow 3d\ ^2D_{3/2,5/2}$. Therefore, corrections for such shifts should be considered for these clock transitions if a tunable laser operating in the infrared or visible regions is used to trap Sc^{2+}. It can be noted that the polarizabilities of the $3d\ ^2D_{3/2,5/2}$ states are changed by a maximum amount of around 10% at $\omega = 0.125$ a.u. from the corresponding static values. On the other hand, this change is around 110% in the polarizability of $4s\ ^2S_{1/2}$ state. Nevertheless, both Fig. 7 and Fig. 8 show some intersections in or very close to the region from $\omega = 0.275$ a.u. to $\omega = 0.300$ a.u. Here we consider those intersections where all the curves in both the figures tend toward zero value with increasing ω. These intersections, as observed in the vacuum ultraviolet (VUV) region, provide the magic wavelengths for the corresponding transitions. With the accessibility of tunable coherent radiation sources in the VUV region [16–21], it may be possible to determine these magic wavelengths experimentally. The positions of the magic wavelengths are found to be very close to the first excitation energies of the $3d\ ^2D_{3/2,5/2}$ states. Therefore, the polarizabilities of the $3d$

TABLE III. Present transition energies in a.u. calculated using the DF and RCCSD(T) theories. The experimental results from the NIST in a.u. [14] are compared.

Transitions	DF	RCCSD(T)	NIST
$4s\ ^2S_{1/2}$–$4p\ ^2P_{1/2}$	0.1595	0.1674	0.1666
$4s\ ^2S_{1/2}$–$4p\ ^2P_{3/2}$	0.1615	0.1696	0.1687
$3d\ ^2D_{3/2}$–$4p\ ^2P_{1/2}$	0.2399	0.2800	0.2830
$3d\ ^2D_{3/2}$–$4p\ ^2P_{3/2}$	0.2419	0.2822	0.2851
$3d\ ^2D_{3/2}$–$4f\ ^2F_{5/2}$	0.5664	0.6211	0.6236
$3d\ ^2D_{5/2}$–$4p\ ^2P_{3/2}$	0.2411	0.2811	0.2842
$3d\ ^2D_{5/2}$–$4f\ ^2F_{5/2}$	0.5656	0.6200	0.6227
$3d\ ^2D_{5/2}$–$4f\ ^2F_{7/2}$	0.5656	0.6200	0.6227

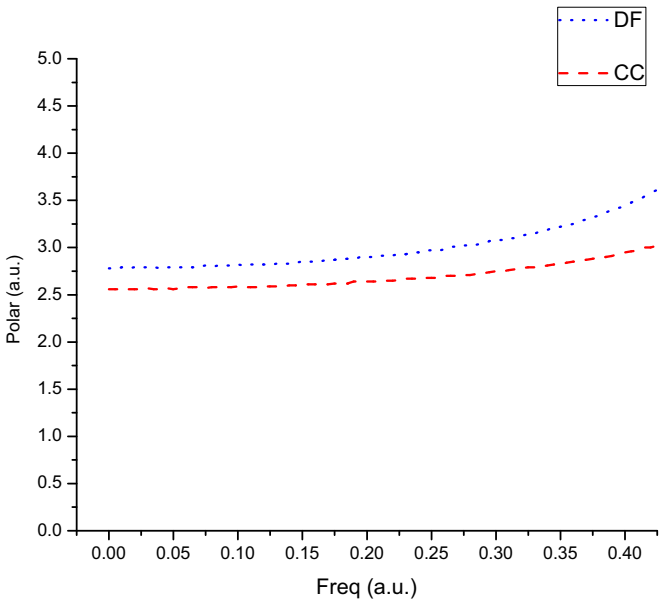

FIG. 6. (Color online) Frequency (Freq) dependence of polarizability (Polar) for the $3d\ ^2D_{5/2}$ state with $M = \pm 5/2$.

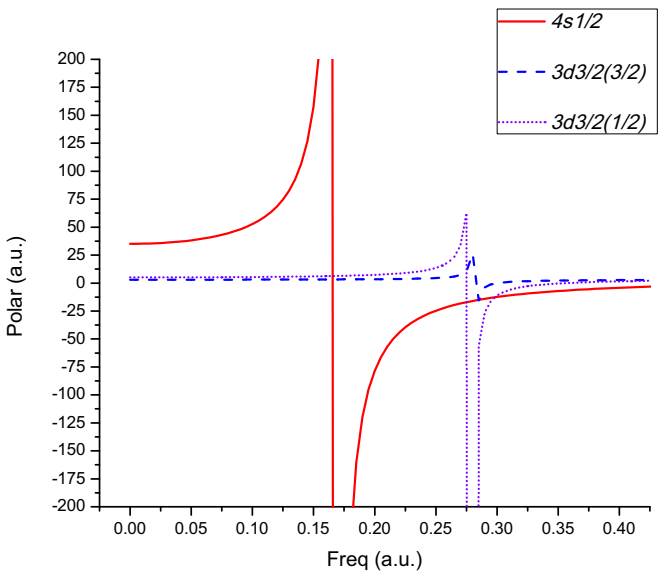

FIG. 7. (Color online) Frequency (Freq) dependence of polarizabilities (Polar) for the $4s\ ^2S_{1/2}$ and $3d\ ^2D_{3/2}$ states at CC level. The brackets indicate the magnitudes of the M components.

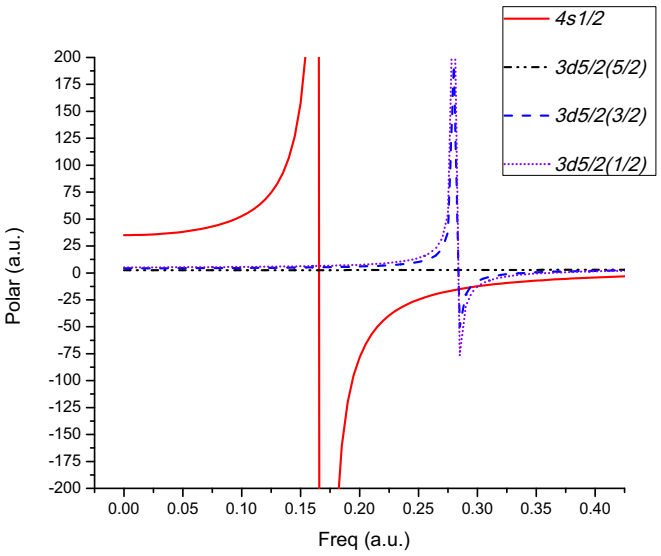

FIG. 8. (Color online) Frequency (Freq) dependence of polarizabilities (Polar) for the $4s\ ^2S_{1/2}$ and $3d\ ^2D_{5/2}$ states at CC level. The brackets indicate the magnitudes of the M components.

$^2D_{3/2,5/2}$ states at these wavelengths are strongly dominated by the terms with the $3d\ ^2D_{3/2,5/2}$–$4p\ ^2P_{1/2,3/2}$ dipole matrix elements. Also, at this frequency region, the polarizabilities of the $4s\ ^2S_{1/2}$ state are dominated by the terms having $4s\ ^2S_{1/2}$–$4p\ ^2P_{1/2,3/2}$ dipole matrix elements. Therefore, as is obvious from Eq. (2.5), Eq. (2.6), and Eq. (2.7), equality of the polarizabilities at the magic wavelengths can be used to determine the $4s\ ^2S_{1/2}$–$4p\ ^2P_{1/2,3/2}$ and $3d\ ^2D_{3/2,5/2}$–$4p\ ^2P_{1/2,3/2}$ transition strengths within a very good level of approximation. One can use the RCCSD(T) data for $3d\ ^2D_{3/2,5/2}$–$4f\ ^2F_{5/2,7/2}$ transition matrix elements as presented in Table I and RCCSD(T) or NIST transition energy values as presented in Table III to do this job. This follows from the fact that the next significant contributions to the valence parts of the $3d\ ^2D_{3/2,5/2}$ polarizabilities at the magic wavelengths appear from the terms having these matrix elements. Nevertheless, the experimental detection of the magic wavelengths can be considered as one of the excellent applications of a tunable radiation source in the VUV region as discussed here. In Table IV, we give the values of the magic wavelengths calculated at the CC and CC(Expt.) levels. We recommend the values of CC(Expt.) as these are determined in a more accurate way by including the experimental transition energies.

TABLE IV. Values of the magic wavelengths in the unit of Å. The labels in parentheses indicate the magnetic sublevels of the corresponding states. The uncertainties in the magic wavelengths are estimated to be around ±0.4%.

Transitions	CC	CC (Expt.)
$3d\ ^2D_{3/2}$ (±1/2)–$4s\ ^2S_{1/2}$	1529	1509
$3d\ ^2D_{3/2}$ (±3/2)–$4s\ ^2S_{1/2}$	1598	1581
$3d\ ^2D_{5/2}$ (±1/2)–$4s\ ^2S_{1/2}$	1516	1496
$3d\ ^2D_{5/2}$ (±3/2)–$4s\ ^2S_{1/2}$	1552	1534

In order to give an approximate estimate of uncertainty in the calculation of a static polarizability value, we consider a few things: (a) uncertainty in $\alpha(0)_c$, (b) uncertainty in the Part I region of $\alpha(0)_v$, (c) uncertainty due to incomplete correlation correction in the Part II region of $\alpha(0)_v$, and (d) uncertainty due to the use of the DF approximation in the Part III region of $\alpha(0)_v$. These are the main sources of error. To estimate the uncertainty (a), we apply our present technique as presented in Eq. (2.4) to calculate the core polarizability of Ca^{2+}, which appears next to Sc^{3+} in the Ar-isoelectronic sequence. We then estimate the percentage differences of this calculated polarizability of Ca^{2+} from the experimental value of Öpik [58] and from the perturbed relativistic coupled-cluster (PRCC) result of Chattopadhaya *et al.* [59]. We take the maximum of these two percentage differences as the uncertainty in the polarizability for Ca^{2+}. We approximate the uncertainty for Sc^{3+} core in (a) to be the same as estimated for the Ca^{2+} core. The uncertainties in (b) can arise from the uncertainties of $4s\ ^2S_{1/2}$–$4p\ ^2P_{1/2,3/2}$ matrix elements for the $4s\ ^2S_{1/2}$ state and $3d\ ^2D_{3/2,5/2}$–$4p\ ^2P_{1/2,3/2}$ matrix elements for the $3d\ ^2D_{3/2,5/2}$ states as the terms associated with these matrix elements dominate here. A significant amount of uncertainty in (c) and (d) can appear in the polarizabilities of $3d\ ^2D_{3/2,5/2}$ states. This is due to the fact that the dipole matrix elements between $3d\ ^2D_{3/2,5/2}$ and $nf\ ^2F_{5/2,7/2}$ states do not converge rapidly with increasing n. Therefore, the sum of the terms associated with these types of matrix elements for $n > 5$ can contribute noticeably. This is shown well in the polarizability calculations of Ca^+ using the SDpT method in Refs. [24,60]. We take the dipole matrix elements of Safronova *et al.* [15] calculated by the SDpT excitations method for $n = 6,7$ of Sc^{2+}. Then the contributions from the terms associated with these matrix elements to the polarizabilities are estimated. However, for other higher n values, the SDpT results are not available in their work [15]. Therefore, we scaled the contributions for these n values with respect to the corresponding SDpT results for Ca^+ [24,60]. Then we recalculate the polarizabilities using this new set of values at Part II and Part III. The differences between the present polarizabilities in Table II and these recalculated polarizibilities are estimated as uncertainties from (c) and (d). All the major sources of errors described in (a), (b), (c), and (d) are summed up to estimate the total uncertainties. The uncertainties in the magic wavelengths also depend on the uncertainties in the $4s\ ^2S_{1/2}$–$4p\ ^2P_{1/2,3/2}$ and $3d\ ^2D_{3/2,5/2}$–$4p\ ^2P_{1/2,3/2}$ matrix elements due to the dominance of the associated terms at these wavelengths. Uncertainty in the core polarizability has no significance here as it is cancelled in the differences of the two polarizabilities. We calculate the uncertainties in the magic wavelengths by checking the maximum variations in the positions of polarizability intersections corresponding to the maximum variations in these matrix elements as quoted in Table I.

Table V and Table VI represent the hyperfine-structure constants A and B, respectively, for $^{45}Sc^{2+}$ as calculated using the DF and RCCSD(T) theories. Without considering isotopic effect, the hyperfine values of the other nearby isotopes can be determined well from the present data through proper scaling by g_I and Q values. We use the Fermi type of nuclear charge distribution function to calculate the hyperfine constants. The electron correlation plays a significant role

TABLE V. Hyperfine A constants for $^{45}Sc^{2+}$ in MHz calculated using the DF and RCCSD(T) theories. $g_I = 1.3590$ is used [61]. The values in parentheses indicate the uncertainties in the RCCSD(T) calculations. "Other" represents the RLCMBPT values [62] and the experimentally measured values [63] in MHz.

State	DF	RCCSD(T)	%Corr	Other[a]	Other[b]
$3d\ ^2D_{3/2}$	296.13	357.13 (±0.5%)	20.60		
$3d\ ^2D_{5/2}$	126.14	84.61 (±4.0%)	−32.92		
$4s\ ^2S_{1/2}$	3916.50	5045.38 (±0.5%)	28.82	4958	5040
$4p\ ^2P_{1/2}$	801.90	1053.71 (±0.5%)	31.40		1050
$4p\ ^2P_{3/2}$	154.66	216.53 (±0.5%)	40.00		210
$4d\ ^2D_{3/2}$	51.21	57.41 (±1.0%)	12.11		
$4d\ ^2D_{5/2}$	21.87	27.32 (±0.5%)	24.92		
$4f\ ^2F_{5/2}$	1.94	2.27 (±0.5%)	17.01		
$4f\ ^2F_{7/2}$	1.08	0.04 (±50.0%)	−96.30		

[a]Reference [62].
[b]Reference [63].

here. The percentage values of the correlations (%Corr) are quoted in the fourth column of both these tables. Unlike the A values, the %Corr seems to affect the hyperfine B constants of the fine-structure states having the same n and L values but different J values by almost the same amount. The B constants of the $4f\ ^2F_{5/2,7/2}$ states are found to be abnormally correlated. These hyperfine values can be substituted in Eq (2.8) to calculate the hyperfine shift of an energy level with a known quantum number F. The sum of the Breit and some of the QED corrections, which are neglected in the present calculations, along with the changes in the results with increasing number of active orbitals and symmetries can provide good estimates of uncertainties in these constants. The present results for the A constants are compared with the other values as found in the literature. We find a very good agreement of our RCCSD(T) results with the measured values of Kopfermann *et al.* [63]. The theoretical value for the $4s\ ^2S_{1/2}$ state was calculated earlier using the relativistic linked-cluster many-body perturbation theory (RLCMBPT). This theory excludes the correlation correction in the wave function beyond the second order [62]. However, the higher-order correlation corrections in the RMBPT are included in this work using the formalism of the RCCSD(T) approach. The $\langle r^{-3}\rangle$ value for the [Ar]$3d$ electronic configuration of Sc^{2+} ion is reported as 1.5755 a.u. in Ref. [64]. Our present calculations for the B constants correspond to the $\langle r^{-3}\rangle$ values 1.5475 a.u. and 1.5378 a.u. for the [Ar]$3d_{3/2}$ and [Ar]$3d_{5/2}$ configurations, respectively.

TABLE VI. Hyperfine B constants for $^{45}Sc^{2+}$ in MHz calculated using the DF and RCCSD(T) theories. $Q = -0.22$ barns is used [61]. The values in parentheses indicate the uncertainties in the RCCSD(T) calculations.

State	DF	RCCSD(T)	%Corr
$3d\ ^2D_{3/2}$	−29.61	−32.00 (±1.0%)	8.07
$3d\ ^2D_{5/2}$	−41.93	−45.42 (±1.0%)	8.32
$4p\ ^2P_{3/2}$	−46.51	−65.25 (±0.5%)	40.29
$4d\ ^2D_{3/2}$	−5.12	−7.72 (±1.0%)	50.78
$4d\ ^2D_{5/2}$	−7.27	−10.96 (±1.0%)	50.76
$4f\ ^2F_{5/2}$	−0.32	−2.77 (±4.0%)	765.63
$4f\ ^2F_{7/2}$	−0.38	−3.23 (±4.0%)	750.00

IV. CONCLUSION

The present calculations of the dynamic polarizabilities can be used to estimate blackbody radiation shifts and frequency-dependent Stark shifts in the $4s\ ^2S_{1/2}$–$3d\ ^2D_{3/2,5/2}$ clock transitions in Sc^{2+}. The magic wavelengths corresponding to these transitions are found at 1496 Å, 1509 Å, 1534 Å, and 1581 Å by our present method. If these magic wavelengths are accurately measured, experimentalists could determine the $3d\ ^2D_{3/2,5/2}$–$4p\ ^2P_{1/2,3/2}$ and $4s\ ^2S_{1/2}$–$4p\ ^2P_{1/2,3/2}$ transition strengths in the future. The present hyperfine-structure constants provide valuable data for accurate line-profile analysis of astrophysically important transition lines and hence can resolve the abundance anomaly issues for scandium.

ACKNOWLEDGMENTS

We are very much thankful to Professor B. P. Das, Indian Institute of Astrophysics, Bangalore, India for valuable discussions regarding polarizability calculations using the RMBPT approach. We are grateful to him, Professor R. K. Chaudhuri, Indian Institute of Astrophysics, Bangalore, India, and Dr. B. K. Sahoo, Physical Research Laboratory, Ahmedabad, India for providing the COUPLED-CLUSTER code. The computations were carried out on the VIRGO cluster at Indian Institute of Technology Madras, Chennai, India. We would like to recognize the funding support from the Department of Science and Technology (DST), Government of India under Project No. SR/S2/LOP-0038/2010-I.

[1] A. Derevianko and H. Katori, Rev. Mod. Phys. **83**, 331 (2011).
[2] M. S. Safronova, V. A. Dzuba, V. V. Flambaum, U. I. Safronova, S. G. Porsev, and M. G. Kozlov, Phys. Rev. Lett. **113**, 030801 (2014).
[3] L. Lorini *et al.*, Eur. Phys. J. Spec. Top. **163**, 19 (2008).
[4] A. Derevianko, V. A. Dzuba, and V. V. Flambaum, Phys. Rev. Lett. **109**, 180801 (2012).
[5] C. W. Chou, D. B. Hume, J. C. J. Koelemeij, D. J. Wineland, and T. Rosenband, Phys. Rev. Lett. **104**, 070802 (2010).
[6] H. G. Dehmelt, IEEE Trans. Instrum. Meas. **IM-31**, 83 (1982).
[7] D. J. Wineland, W. M. Itano, J. C. Bergquist, and R. G. Hulet, Phys. Rev. A **36**, 2220 (1987).
[8] J. C. Berengut, V. A. Dzuba, V. V. Flambaum, and A. Ong, Phys. Rev. A **86**, 022517 (2012).
[9] Matsubara *et al.*, Opt. Express **20**, 22034 (2012).
[10] C. Champenois, M. Houssin, C. Lisowski, M. Knoop, G. Hagel, M. Vedel, and F. Vedel, Phys. Lett. A **331**, 298 (2004).

[11] M. Kajita, Y. Li, K. Matsubara, K. Hayasaka, and M. Hosokawa, Phys. Rev. A **72**, 043404 (2005).

[12] H. S. Margolis, G. P. Barwood, G. Huang, H. A. Klein, S. N. Lea, K. Szymaniec, and P. Gill, Science **306**, 1355 (2004).

[13] A. A. Madej, J. E. Bernard, P. Dubé, L. Marmet, and R. S. Windeler, Phys. Rev. A **70**, 012507 (2004).

[14] A. Kramida, Yu. Ralchenko, J. Reader, and NIST ASD Team (2014), *NIST Atomic Spectra Database* (ver. 5.2) [online], available at http://physics.nist.gov/asd, National Institute of Standards and Technology, Gaithersburg, MD.

[15] M. S. Safronova and U. I. Safronova, Phys. Rev. A **85**, 022504 (2012).

[16] G. Hilber, A. Lago, and R. Wallenstein, *Laser Spectroscopy VIII*, Springer Series in Optical Sciences, edited by W. Persson, and S. Svanberg (Springer, Berlin Heidelberg, 1987), Vol. 55, p. 446.

[17] B. P. Stoicheff, *Frontiers of Laser Spectroscopy of Gases*, NATO Advanced Studies Institute Series, edited by A. C. P. Alves, J. M. Brown, and J. M. Hollas (Springer, Netherlands, 1988), Vol. 234, p. 63.

[18] C. Tian, P. Wang, and T. Sun, Opt. Commun. **100**, 204 (1993).

[19] K. Yamanouchi and S. Tsuchiya, J. Phys. B **28**, 133 (1995).

[20] T. Uchimura, T. Onoda, C.-H. Lin, and T. Imasaka, Rev. Sci. Instrum. **70**, 3254 (1999).

[21] R. H. Lipson, S. S. Dimov, P. Wang, Y. J. Shi, D. M. Mao, X. K. Hu, and J. Vanstone, Vacuum ultraviolet and extreme ultraviolet lasers: Principles, Instrumentation, and Applications, Instrum. Sci. Technol. **28**, 85 (2007).

[22] J. Mitroy, M. S. Safronova, and C. W. Clark, J. Phys. B **43**, 202001 (2010).

[23] M. S. Safronova, M. G. Kozlov, and C. W. Clark, IEEE Trans. Ultrason. Ferroelectr. Freq. Control **59**, 439 (2012).

[24] M. S. Safronova and U. I. Safronova, Phys. Rev. A **83**, 012503 (2011).

[25] D. Jiang, B. Arora, M. S. Safronova, and C. W. Clark, J. Phys. B **42**, 154020 (2009).

[26] Y.-B. Tang, H.-X. Qiao, T.-Y. Shi, and J. Mitroy, Phys. Rev. A **87**, 042517 (2013).

[27] C. Cormick, T. Schaetz, and G. Morigi, New J. Phys. **13**, 043019 (2011).

[28] Ch. Schneider, M. Enderlein, T. Huber, and T. Schaetz, Nat. Photon. **4**, 772 (2010).

[29] J. Eschner, G. Morigi, F. Schmidt-Kaler, and R. Blatt, J. Opt. Soc. Am. B **20**, 1003 (2003).

[30] T. P. Snow and S. L. Dodgen, Astrophys. J. **237**, 708 (1980).

[31] G. Massacrier and M.-C. Artru, Astron. Astrophys. **538**, A52 (2012).

[32] P. E. Nissen, Y. Q. Chen, W. J. Schuster, and G. Zhao, Astron. Astrophys. **353**, 722 (2000).

[33] T. Andersen, P. Petersen, and E. Biemont, J. Quant. Spectrosc. Radiat. Transfer **17**, 389 (1977).

[34] F. LeBlanc and G. Alecian, Astron. Astrophys. **477**, 243 (2008).

[35] C. Huang, G. Zhao, H. W. Zhang, and Y. Q. Chen, Mon. Not. R. Astron. Soc. **363**, 71 (2005).

[36] Y. Takeda, Publ. Astron. Soc. Jpn. **59**, 335 (2007).

[37] E. Biemont, J. Quant. Spectrosc. Radiat. Transfer **16**, 137 (1976).

[38] M. S. Dimitrijević and S. Sahal-Bréchot, Astron. Astrophys. Suppl. Ser. **95**, 121 (1992); **131**, 143 (1998).

[39] P. Villemoes, R. van Leeuwen, A. Arnesen, F. Heijkenskjöld, A. Kastberg, M. O. Larsson, and S. A. Kotochigova, Phys. Rev. A **45**, 6241 (1992).

[40] M. G. Edmunds, Astron. Astrophys. **23**, 311 (1973).

[41] D. C. Morton, Astrophys. J., Suppl. Ser. **149**, 205 (2003).

[42] A. M. Sossah, H.-L. Zhou, and S. T. Manson, Phys. Rev. A **78**, 053405 (2008).

[43] J. Zeng, G. Zhao, and J. Yuan, Phys. Rev. A **68**, 022714 (2003).

[44] D. K. Nandy, Y. Singh, B. K. Sahoo, and C. Li, J. Phys. B **44**, 225701 (2011).

[45] J. X. Prochaska and A. McWilliam, Astrophys. J. **537**, L57 (2000).

[46] L. Young, W. J. Childs, T. Dinneen, C. Kurtz, H. G. Berry, L. Engström, and K. T. Cheng, Phys. Rev. A **37**, 4213 (1988).

[47] R. K. Chaudhuri, B. K. Sahoo, B. P. Das, H. Merlitz, U. S. Mahapatra, and D. Mukherjee, J. Chem. Phys. **119**, 10633 (2003).

[48] I. Lindgren and J. Morrison, in *Atomic Many-body Theory*, edited by G. E. Lambropoulos and H. Walther (Springer, Berlin, 1985), Vol. 3.

[49] G. Dixit, B. K. Sahoo, R. K. Chaudhuri, and S. Majumder, Phys. Rev. A **76**, 042505 (2007).

[50] I. Lindgren and D. Mukherjee, Phys. Rep. **151**, 93 (1987).

[51] S. Pal, M. Rittby, R. J. Bartlett, D. Sinha, and D. Mukherjee, Chem. Phys. Lett. **137**, 273 (1987); J. Chem. Phys. **88**, 4357 (1988).

[52] T. K. Ghosh, A. K. Das, M. Castro, S. Canuto, and P. K. Mukherjee, Phys. Rev. A **48**, 2686 (1993).

[53] W. R. Johnson, Z. W. Liu, and J. Sapirstein, At. Data Nucl. Data Tables **64**, 279 (1996).

[54] K. T. Cheng and W. J. Childs, Phys. Rev. A **31**, 2775 (1985).

[55] G. Dixit, H. S. Nataraj, B. K. Sahoo, R. K. Chaudhuri, and S. Majumder, Phys. Rev. A **77**, 012718 (2008).

[56] F. A. Parpia, C. F. Fischer, and I. P. Grant, Comput. Phys. Commun. **175**, 745 (2006).

[57] C. Sur, B. K. Sahoo, R. K. Chaudhuri, B. P. Das, and D. Mukherjee, Eur. Phys. J. D **32**, 25 (2005).

[58] U. Öpik, Proc. Phys. Soc. **92**, 566 (1967).

[59] S. Chattopadhyay, B. K. Mani, and D. Angom, Phys. Rev. A **87**, 062504 (2013).

[60] B. Arora, M. S. Safronova, and C. W. Clark, Phys. Rev. A **76**, 064501 (2007).

[61] P. Raghavan, At. Data Nucl. Data Tables **42**, 189 (1989).

[62] A. Owusu, X. Yuan, S. N. Panigrahy, R. W. Dougherty, T. P. Das, and J. Andriessen, Phys. Rev. A **55**, 2644 (1997).

[63] H. Kopfermann and H. Wittke, Z. Phys. **105**, 16 (1937).

[64] B. A. Goodman and J. B. Raynor, J. Inorg. Nucl. Chem. **32**, 3406 (1970).